J Solid State Electrochem (2012) 16:1487–1492
DOI 10.1007/s10008-011-1547-9

ORIGINAL PAPER

Synergistic effect of additives on electrochemical properties of MnO_2 cathode in aqueous rechargeable batteries

Manickam Minakshi · Pritam Singh

Received: 24 July 2011 / Revised: 30 August 2011 / Accepted: 3 September 2011 / Published online: 30 September 2011

Abstract The synergistic effect of bismuth oxide (Bi_2O_3) + titanium disulphide (TiS_2) additives in different proportions into the MnO_2 cathode material is physically modified and tested in a Zn-MnO_2 battery with aqueous LiOH electrolyte. It is found that these foreign cations stabilized the MnO_2 structure upon multiple cycling and the synergistic effect between two additives enhanced the rechargeability. This class of additive modified MnO_2 may be of interest for high-energy density and safer batteries for applications such as electric vehicles. The cyclability of the material suitable for electric vehicle (EV) applications is established in this report. The incorporation of Bi_2O_3 (3 wt.%) and TiS_2 (2 wt.%) additives into the MnO_2 cathode was found to improve the cell performance, this is partly due to the suppression of proton insertion. The results on cyclic voltammetric and charge–discharge studies describing the redox mechanisms in LiOH electrolyte and the role of additives on those redox reactions are discussed and compared with that of traditional KOH electrolyte.

Keywords Additives · Synergistic · Bismuth · Titanium · MnO_2

Introduction

With the rapid development of modern electronic devices and the realization that fossil fuels are almost depleting, the demand for an alternative energy resource is rising [1]. In this aspect, the electrochemical storage of energy by means of rechargeable batteries and/or fuel cells shows a tremendous potential of growth [2]. Issues such as the environment, the rapid increase in fossil fuel prices and its relative scarcity, and the increased deployment of renewable energy sources, provide a greater need for the development of electrochemical energy storage, especially for electric vehicle applications [1, 2]. Progress will strongly depend on the development of new, improved materials suitable for higher energy storage [3]. Thus, solid-state (materials) research plays a key role in making further progress in the field of energy storage. Various primary and secondary batteries have been developed over the years. A major concern is the environmental threat posed by the highly toxic Pb, Ni and Cd type electrodes, and highly corrosive H_2SO_4 and KOH as the electrolytes with a meagre energy density [4]. Lithium ion batteries have excellent energy density of any of the commonly available rechargeable batteries [5]. However, the chemical reactivity constraints necessitated development of suitable non-aqueous (organic) electrolytes. Organic electrolytes suffer from toxicity, flammability and other safety issues [6, 7]. In addition, due to a water-free fabrication environment and the high costs of organic solvents, the manufacturing costs are also high. As society is getting more aware of these issues, the desire for environmentally friendly battery components is required.

The zinc-manganese dioxide battery is the most commonly known primary (non rechargeable) battery that dominates the primary battery segment [8]. Existing non-rechargeable Zn/MnO_2 battery uses an alkaline KOH electrolyte [9]. These cells are based on the insertion of protons (H^+) into MnO_2 resulting in a non-reversible process [9]. Our earlier work has shown that using LiOH

M. Minakshi (✉) · P. Singh
Faculty of Minerals and Energy, Murdoch University,
Murdoch, WA 6150, Australia
e-mail: minakshi@murdoch.edu.au

M. Minakshi
e-mail: lithiumbattery@hotmail.com

as an electrolyte can result in the insertion of Li ions into MnO_2 [10, 11]. This has the potential to lead to a new field of rechargeable alkaline batteries sustaining hundreds of cycles. Furthermore, lithium aqueous electrolytes have ion conductivities about two orders of magnitude higher than their non-aqueous counterparts, so thick electrodes can be used in our system in order to increase power. Such high power cells offer great potential in electric vehicles (EV) applications. In continuation to this research, our studies have shown that lithium intercalation can occur in the electrodes immersed in aqueous lithium electrolytes and the operating characteristics are desirable [10, 11]. During the battery discharge, mechanism involves both lithium and proton intercalation into the host MnO_2 compound. The intake of proton insertion results in manganese oxy hydroxide (MnOOH) as the discharged product. This MnOOH is not reversible for multiple cycles, hence resulted an unwanted discharged product. The correlation between additives incorporated into the cathode and the suppression of unwanted discharge products could improve the rate capability of this battery. Interestingly, our earlier studies showed that the incorporation of additives such as TiB_2, CeO_2, MgO, B_4C or Bi_2O_3 compounds in a suitable proportion into physically modified MnO_2 lead to an enhanced battery performance [12–16]. These factors have been identified as being the likely bottlenecks in developing the Zn/MnO_2 aqueous rechargeable battery technology. In this report, we have studied the individual effect of titanium disulphide (TiS_2) and bismuth oxide (Bi_2O_3) and the synergistic effect of these additives in the MnO_2 cathode using the potentiostatic and galvanostatic techniques.

Experimental

The EMD (electrolytic manganese dioxide) of γ-MnO_2 type (IBA sample 32) material used in this work was purchased from the Kerr McGee Chemical Corporation. Bismuth oxide (Bi_2O_3) and titanium disulphide (TiS_2) was obtained from Aldrich Chemical and Alfa Aesar, respectively. For cyclic voltammetric (CV) experiments, a standard three-electrode cell was used. For this purpose, the γ-MnO_2 working electrode was made as follows: γ-MnO_2 powder (with 5 wt.% of additives [Bi_2O_3, TiS_2, or Bi_2O_3 + TiS_2]) was pressed on to a disc of Pt gauze. On the other side of a disc, a layer of conductive carbon (A-99, Asbury USA) was also pressed. The MnO_2 side of the disc was exposed to the LiOH electrolyte through a Teflon barrel. For making electrical connection of MnO_2 a Pt disc was inserted into the barrel on top of the carbon side which contacted a stainless steel plunger. The counter-electrode was a zinc foil, which was separated from the main electrolyte by means of a porous frit. A mercury–mercuric oxide (Hg/HgO) served as the reference electrode. Reported potentials are relative to Hg/HgO. The electrolyte was 5 M concentrations of aqueous lithium or potassium hydroxide electrolytes. The working electrode was cycled between 0.2 and −0.45 V at a slow scan rate of 25 μV s^{-1} scan rate. On each occasion, the potential scan started at 0.2 V, moving initially in the cathodic direction and then reversed back anodically to the starting point.

For battery (galvanostatic) experiments, a Swagelok type two cell electrode was used. The γ-MnO_2 active material was first mixed with 5 wt.% of suitable additives (Bi_2O_3, TiS_2, or Bi_2O_3 + TiS_2), 15 wt.% of carbon black and with 10 wt.% of poly(vinylidene difluoride) (PVDF, Sigma Aldrich) as a binder and then pressed into a disc shape with a diameter of 12 mm. Each disk was 0.3 mm thick and weighed approximately 20 mg. An electrochemical test cell was constructed with the disk as the cathode, Zn metal as the anode and filter paper (Whatman filters 12) as the separator. The cell was discharged/charged galvanostatically using an eight channel battery analyser from Neware, China, operated by a battery testing system (BTS). The cut-off discharge and charge voltages were 1.0 and 1.9 V, respectively. All electrochemical measurements were carried out under ambient temperature.

Results and discussion

To understand the electrochemical behaviour of the γ-MnO_2 in aqueous electrolytes, a slow scan cyclic voltammetry is deployed. The effect of replacing KOH with LiOH electrolyte was determined by carrying out redox cycles on two identical cells, one containing 5 M LiOH and other 5 M KOH. Figure 1 shows the first cyclic voltammogram (CV) of γ-MnO_2 in LiOH can be compared to that in KOH under the conditions noted in the figure. It is evident that

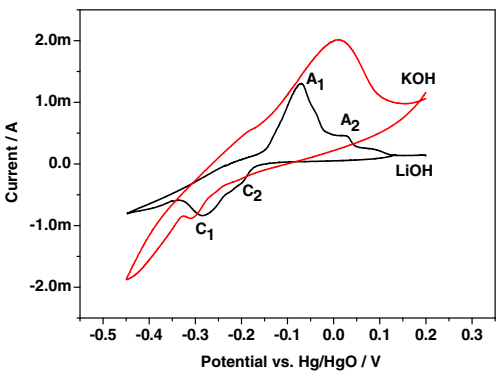

Fig. 1 Cyclic voltammogram for plain MnO_2 electrode in 5 M concentrations of LiOH and KOH electrolytes. Voltage was swept cathodically initially from +0.2 to −0.45 V and back at a scan rate of 25 μV s^{-1}

the CVs of MnO_2 in the two electrolytes appear to be quite different. This prompted us to study the redox mechanism and electrochemical phenomenon involved in the different aqueous electrolyte batteries that will enhance scientific understanding of aqueous rechargeable batteries.

The CV for MnO_2 in LiOH electrolyte consists of a well defined reduction peak C_1 at −0.28 V, which corresponds to the mechanism of the intercalation of lithium. On reversing the cycle, a corresponding anodic peak A_1 at −0.07 V of identical behaviour represents that the electrochemical process (Eqs. 1 and 2) is reversible. A small shoulder at 0.03 V is also seen during scanning in the anodic direction, implying that the oxidation occurs in two steps: formation of MnO_2 (peak A1) and Mn_3O_4 (peak A2). A CV for MnO_2 in KOH electrolyte is superimposed in Fig. 1. Compared with the voltammogram for LiOH electrolyte, the behaviour of the cell with KOH electrolyte appears to have only an oxidation peak A_1 (0.01 V) with an increase in area under the peak and current but without a well defined reduction peak C_1 (−0.3 V). This may be due to a mild concentration of KOH, however, while sweeping to more negative potential (−0.7 V vs. Hg/HgO) the electrochemical process become irreversible. Hence, we have chosen between + 0.2 and −0.35 V as a safe voltage window for our continuous cycling experiments. Based on what is reported in the literature [9, 17, 18], for KOH electrolyte the sharp drop in current during the reduction process (at −0.4 V vs. Hg/HgO) corresponds to the proton intercalation. Protons originating from the water of the KOH electrolyte are inserted into the host MnO_2 pertaining to the formation of MnOOH and $Mn(OH)_2$ [19, 20]. On subsequent oxidation, $Mn(OH)_2$ is oxidised to a variety of Mn^{3+} intermediates, including, birnessite MnO_2 and Mn_3O_4 [20]. In contrast to this fact, in one of our earlier reports, we noted [21] that besides proton, K^+ insertion is also evidenced for KOH electrolyte, corresponding to the tiny reduction peak C1 (−0.3 V) seen in Fig. 1. The difference of 20 mV seen in the reduction C1 peaks between the two electrolytes is attributed to the Li^+ and K^+ intercalation mechanism. Either proton or potassium-ion insertion in both the cases the redox process is not reversible with KOH electrolyte [9, 21]. For LiOH electrolyte the peak C_1 at −0.28 V, the reaction mechanism suggested by our group earlier [12–16], corresponds to the formation of lithium-intercalated MnO_2 phase but the case is not that simple as observed from the cyclability (in Fig. 2). The materials that are formed at the end of the reduction process examined by XRD showed [12, 16] a mixture of phases involving both lithium and proton intercalation (as shown in Eq. 1).

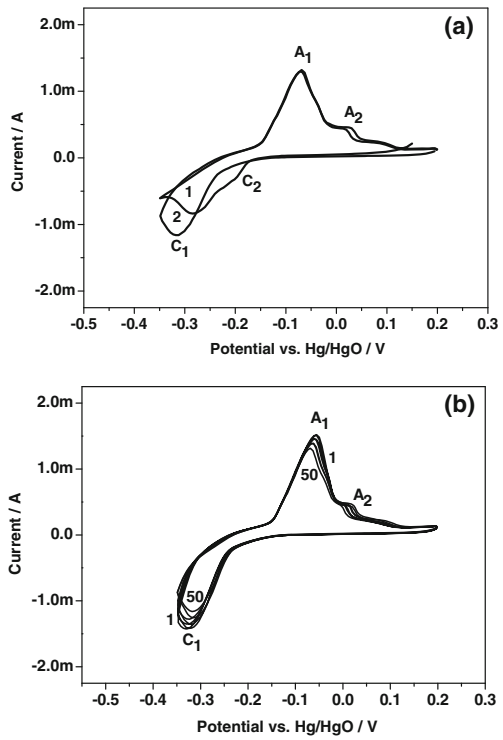

Fig. 2 Cyclic voltammogram for plain MnO_2 electrode for the **a** initial two and **b** multiple cycles in 5 M LiOH electrolyte. Voltage was swept cathodically initially from +0.2 to −0.35 V and back at a scan rate of 25 μV s^{-1}. Cycle numbers are indicated in the figure for LiOH cell

$$Zn + 2MnO_2 + 2LiOH + 2OH^- + H_2O \rightarrow Zn(OH)_4^{2-} + LiMnO_2 + MnOOH + LiOH \quad (1)$$

$$MnOOH + H^+ + e^- \rightarrow \text{mixture of} \left[Mn_2O_3 + Mn(OH)_2\right] \quad (2)$$

The MnOOH in the electrode undergoes a dissolution reaction that releases Mn^{3+} ions into the electrolyte. The Mn^{3+} species are further reduced to a soluble Mn^{2+} that subsequently precipitates to form the end products as $Mn(OH)_2$. This product is then recharged to a variety of products like MnO_2, birnessite-type MnO_2 and Mn_3O_4 [12]. From these results, it can be concluded that for KOH, the reaction process K^+ ion from the electrolyte into the MnO_2 retards the usual protonation mechanism for reversibility, while for LiOH the redox process is reversible and a new class of cell is reported here.

Figure 2 shows the changes in the CV profile when the MnO_2 material is subjected to continuous cycling (50 cycles) in the same potential region in LiOH electrolyte and compared those with the first two cycles. The reduction peak C_1 at −0.28 V in the second cycle (in Fig. 2a) is shifted more negatively, changed in intensity and its shape to that of the first cycle, illustrating that the electrochemical processes is not fully reproducible. The peak area (in Fig. 2a) for the intercalation mechanism is smaller than the peak area of the first reduction peak at −0.28 V. The cathodic and anodic peak currents decreased considerably,

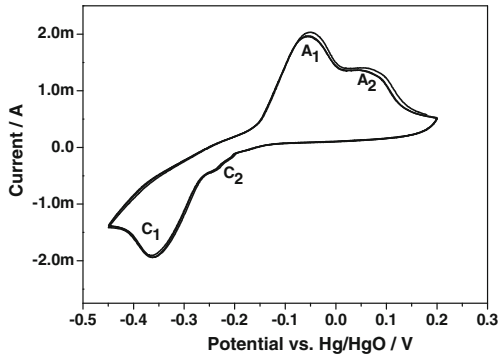

Fig. 3 Cyclic voltammogram for Bi_2O_3 (5 wt.%) modified MnO_2 electrode in 5 M LiOH electrolyte. Voltage was swept cathodically initially from +0.2 to −0.45 V and back at a scan rate of 25 μV s^{-1}

suggesting that the MnO_2 material needs to be improved while eliminating the inactive phases of MnOOH and Mn_3O_4 during the redox process. To be suitable for any practical applications, the electrochemical process needs to be reproducible with acceptable efficiency over multiple cycling for immediate appliances.

To improve the rechargeability while preventing the formation of inactive phases (suppression of proton insertion) during the redox processes, we have introduced a variety of additives such as Bi and Ti cations, which is widely argued in the literature [17, 18, 22, 23] against structure stabilizing effects. However, the synergistic effect of these additives in a right proportion in aqueous rechargeable battery with LiOH electrolyte has never been reported. A CV for MnO_2 with a 5 wt.% Bi_2O_3 additive is shown in Fig. 3. Compared with the voltammogram for plain MnO_2 (Fig. 2), the peak currents of the working electrode with Bi_2O_3 added MnO_2 are increased. The area of the reduction C_1 and oxidation A_1 peaks are higher, suggesting that the reversibility of MnO_2 is enhanced with the presence of Bi cations. The peak A_1 corresponds to the reverse reaction of the lithium-intercalated MnO_2, whereas peak A_2 suggests the oxidation of Mn(OH)2

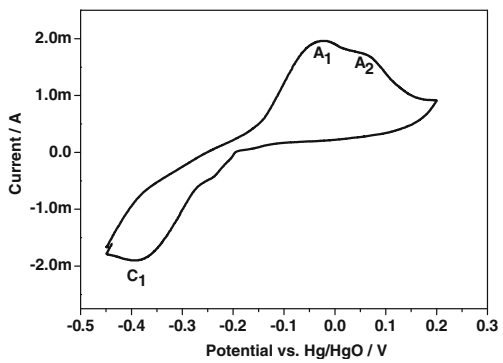

Fig. 4 Cyclic voltammogram for TiS_2 (5 wt.%) modified MnO_2 electrode in 5 M LiOH electrolyte. Voltage was swept cathodically initially from +0.2 to −0.45 V and back at a scan rate of 25 μV s^{-1}

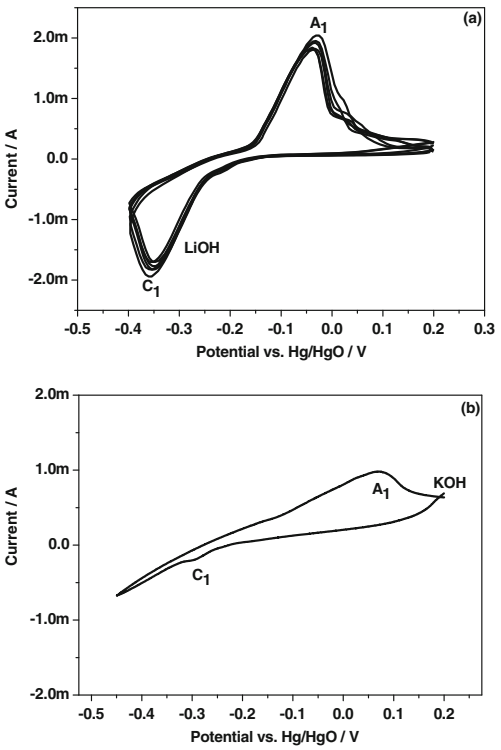

Fig. 5 Cyclic voltammogram for multiple additives Bi_2O_3 (3 wt.%) + TiS_2 (2 wt.%) modified MnO_2 electrode in **a** 5 M LiOH and **b** KOH electrolytes. Voltage was swept cathodically initially from +0.2 to −0.4 V and back at a scan rate of 25 μV s^{-1}

leading to Mn_3O_4. The very important feature in Fig. 3 is that the areas of the peaks are identical for multiple cycling. This indicates that Bi cations have a substantial effect on reversibility, stabilising the structure against the spinel formation [24]; however, the formation of inactive phase Mn_3O_4 is not suppressed. Therefore, it can be concluded that the Bi additive enhances the rechargeability but does not prevent the formation of an inactive phase, showing that the objective of this work is not fully achieved with this additive.

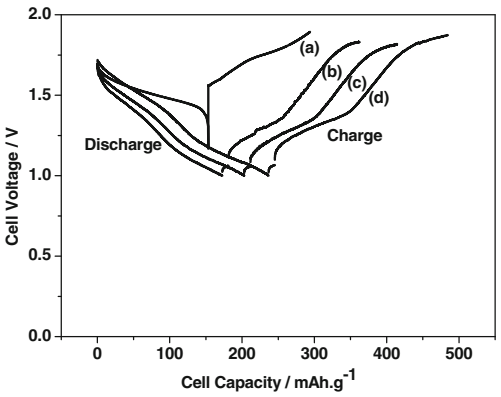

Fig. 6 Constant current discharge–charge curves of Zn|LiOH|MnO_2 battery in the presence and absence of additives. MnO_2 containing **a** 0 wt.%, **b** 5 wt.% Bi_2O_3, **c** 5 wt.% TiS_2, **d** 3 wt.% Bi_2O_3 + 2 wt.% TiS_2 additives

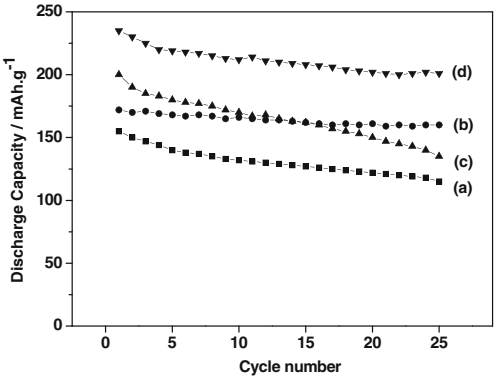

Fig. 7 Cyclability of Zn|LiOH|MnO_2 battery in the presence and absence of additives. MnO_2 containing **a** 0 wt.%, **b** 5 wt.% Bi_2O_3, **c** 5 wt.% TiS_2, **d** 3 wt.% Bi_2O_3 + 2 wt.% TiS_2 additives

Following the incorporation of Bi^{3+}, we tried with Ti^{4+} cations, and the observed CV for TiS_2 (5 wt.%) is shown in Fig. 4. The area of the reduction peak C_1 is slightly decreased and notably the oxidation peak A_2 almost disappeared or at least not well defined to that of Bi added MnO_2 in Fig. 3. The presence of TiS_2 additive is found to prevent the formation of inactive phase Mn_3O_4, but the peak currents are comparatively smaller to that of Bi added MnO_2. To evaluate the synergistic effect on the multiple additives upon the rechargeability of MnO_2 cathode materials, Bi_2O_3 and TiS_2 (at 3 wt.% and 2 wt.%, respectively) have been used and its behavior in LiOH is compared to that in KOH electrolyte by referring to Fig. 5. Interestingly, the results for LiOH electrolyte (Fig. 5a) showed that the incorporation of multiple additives, i.e., TiS_2 or Bi_2O_3, in a suitable proportion into the MnO_2 cathode retards the dissolution reaction (Eqs. 1 and 2) of Mn^{3+} by keeping the Mn^{3+} ions in the solution for a longer period, i.e., during the discharge process, and thereby prevents the formation of unwanted Mn_3O_4. This leads to improved electrochemical performance by the clear elimination of A_2 oxidation peak and the peak currents of the MnO_2 electrode are well increased in intensity. The electrochemical redox process is found to be reversible for multiple cycles. Hence, the synergistic effect of these two additives played a crucial role in suppressing the inactive phase and improving the rechargeability against the MnO_2 lattice stability. However, the presence of the same proportion of these multiple additives in the MnO_2 cathode with KOH electrolyte does not appear to have a pronounced effect (in Fig. 5b). The shape and size of the voltammogram with KOH is very different to that of the LiOH electrolyte. The reduction peak C1 is not well defined due to K^+ ion insertion, and the presence of Mn_3O_4 is not readily observed for the given 5 M concentration of KOH electrolyte. The results reported by Raghuveer and Manthiram [25, 26] demonstrated that the formation of Mn_3O_4 and birnessite MnO_2 phases and the role of additives in influencing the suppression of these phases are viable only under the conditions of using a strong base 9 M KOH electrolyte.

Identification of the mechanism of lithium intercalation into the host MnO_2-based oxide materials and its synergistic effect of additives paved a way for environmental friendly aqueous rechargeable batteries. To validate this material for a battery application, we have carried out galvanostatic tests for multiple cycles.

Figure 6 shows the first cycle discharge–charge characteristics of the Zn/MnO_2 battery compared in the absence and presence of additives and the synergistic effect of these additives with LiOH electrolyte. All the cells could be reversibly discharged and charged. The plain MnO_2 (without any additive) battery shows higher discharge and charge voltage profiles than the additive containing MnO_2 batteries, and this difference is 0.1 and 0.3 V for mid-discharge and mid-charge voltages, respectively. The degree of active material utilization is quite high for the battery containing multiple additives. The discharge capacities for the MnO_2 cathode containing 0 wt.% additive, 5 wt.% Bi_2O_3, 5 wt.% TiS_2, and 3 wt.% Bi_2O_3 + 2 wt.% TiS_2 are calculated to be 155, 170, 200 and 240 mA h/g, respectively. The data indicate that the addition of small amounts of multiple additive led to a significant improvement in the energy storage capacity compared to the individual Bi_2O_3 or TiS_2 additives. The cyclability data (Fig. 7) shows the Zn-MnO_2 battery with LiOH electrolyte is rechargeable but the cathode containing multiple additives holds higher capacity 200 mA h/g even after 25th cycle and retaining excellent energy storage. This concludes that MnO_2 containing Bi_2O_3+ TiS_2 additives can be a potential candidate for aqueous rechargeable batteries.

Conclusions

The electrochemical behaviour of manganese dioxide with aqueous LiOH electrolyte demonstrated the intercalation of lithium ions into the host structure, and their suitability as cathode material in energy storage is of great interest in terms of their high discharge capacity. In the presence of individual and multiple additives, the battery capacity was substantially improved. The key concept and strategy of this work showed the unique property of transforming the primary battery into a high-performance secondary battery while using aqueous lithium hydroxide as an electrolyte. Additives such as Bi_2O_3 are shown to stabilise the MnO_2 structure for reversibility, whereas TiS_2 suppresses the formation of inactive phases. The traditional cell with KOH electrolyte behaves quite differently from the Zn/MnO_2-LiOH cell and the redox mechanism varies in terms of lithium and potassium ion intercalation.

Acknowledgements M. Minakshi wishes to acknowledge the Australian Research Council (ARC) and Centre for Research into Energy for Sustainable Transport (CREST). This research was supported under Australian Research Council's Discovery Projects funding scheme (DP1092543) and CREST (Center of Excellence, Project 1.1.5).

References

1. Chalk SG, Miller JF (2006) J Power Sourc 159:73–80
2. Peng B, Chen J (2009) Coord Chem Rev 253:2805–2813
3. Fichtner M (2011) Conversion materials for hydrogen storage and electrochemical applications—concepts and similarities. J Alloy Comp (in press)
4. Rydh CJ (1999) J Power Sourc 80:21–29
5. Whittingham MS (2004) Chem Rev 104:4271–4302
6. Luo JY, Cui WJ, He P, Xia YY (2010) Nat Chem 2:760–765
7. Sun Y, Jiang S, Bi W, Wu C, Xie Y (2011) Highly ordered lamellar V_2O_3-based hybrid nanorods towards superior aqueous lithium-ion battery performance. J Power Sourc 196:8644–8650
8. Linden D (1995) In: Linden D (ed) Handbook of batteries. McGraw-Hill, New York
9. Kordesch K, Gsellmann J, Peri M, Tomantschger K, Chemelli R (1981) Electrochim Acta 26:1495–1504
10. Minakshi M, Singh P, Issa TB, Thurgate S, DeMarco R (2004) J Power Sourc 130:254–259
11. Minakshi M, Singh P, Mitchell DRG (2007) J Electrochem Soc 154:A109–A113
12. Minakshi M, Mitchell DRG, Prince K (2008) Solid State Ionics 179:355–361
13. Minakshi M, Nallathamby K, Mitchell DRG (2009) J Alloy Comp 479:87–90
14. Minakshi M, Blackford MG, Ionescu M (2011) J Alloy Comp 509:5890–5974
15. Minakshi M, Blackford MG (2010) Mater Chem Phys 123:700–705
16. Minakshi M, Mitchell DRG (2008) Electrochim Acta 53:6323–6327
17. Im D, Manthiram A (2003) J Electrochem Soc 150:A68–A73
18. Yu LT (1997) J Electrochem Soc 144:A802–A809
19. Kozawa A, Yeager JF (1965) J Electrochem Soc 112:A959–A963
20. Kozawa A, Yeager JF (1968) J Electrochem Soc 115:A1003–A1007
21. Minakshi M (2008) J Electroanal Chem 616:99–106
22. Wroblowa HS, Gupta N (1987) J Electroanal Chem 238:93–102
23. Wroblowa HS, Gupta N (1987) J Electroanal Chem 238:107–117
24. Im D, Manthiram A, Coffey B (2003) J Electrochem Soc 150:A1651–A1659
25. Raghuveer V, Manthiram A (2006) J Power Sourc 163:598–603
26. Raghuveer V, Manthiram A (2006) J Power Sourc 159:1468–1473